The poleward shift of the Subtropics in the Northern Hemisphere winter: time of emergence of the climate change signals

Roberta D'Agostino[1],

Ascanio L. Scambiati [2], Johann Jungclaus [1] and Piero Lionello [2,3]

[1] Max-Planck-Institut für Meteorologie, Hamburg, Germany

[2] University of Salento, Lecce, Italy

[3] CMCC, Euro-Mediterranean Center on Climate Change, Lecce, Italy

Max-Planck-Institut für Meteorologie

UNIVERSITÀ DEL SALENTO

cmcc Centro Euro-Mediterraneo sui Cambiamenti Climatici

Poleward shift of subtropical margins

The projected poleward shift of subtropical margins will affect densely populated areas of the Northern Hemisphere that have limited or scarce water resources. Therefore, it is fundamental for societies in these areas to know when the effects of climate change on the regional environment will become apparent, because this information can make the difference for effective adaptation and mitigation strategies. The position of the subtropical margins is intimately related to the zonal-mean Hadley Circulation, but is also affected by regional processes related to the distribution of continents, oceans and to their characteristics. In our study we show that the northward shift of the subtropics has strong regional connotations and only in few areas, e.g. the eastern Mediterranean, Western Asia and, to a lower extent the Western Pacific, the anthropogenic climate change signal will emerge from the natural climate variability before the end of the 21st century.

Submitted to Geophysical Research Letters: D'Agostino et al., 2020

MPI-GE - the Grand Ensemble

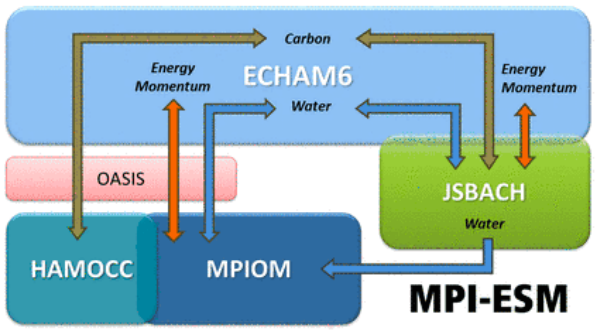

The largest ensemble of a single comprehensive climate model currently available, with 100 members for different forcing scenarios

Experiments:

Pre-industrial control (2,000 model years)
Historical (1850-2005)
RCP2.6
RCP4.5
RCP8.5 (2006-2099)
1% CO^2 (150 years)

Unlike other Large Ensembles (CESM-LE, CESM-ME and CanESM-LE) the initialisation has been made by sampling the pre-industrial control state, which samples the full phase space of both the ocean and the atmosphere states. This produces a larger spread than the atmospheric perturbation method and then it is a better sample of the full variability range from the beginning of the simulation (Hawkins et al., 2016). This allows investigation of the late 19th and early 20th century warming and its effect on Earth's climate.

MPI-GE allows us to quantify the relative role of the internal climate variability against the external forcing, as well as providing an estimated time-of-emergence of forced signal from the noise.

Forced response vs internal variability

The impact of the external forcing here is described by the so-called Forced Response (FR), represented by the variance of the ensemble mean among every ensemble members:

$$F_r^i = \frac{\sum_{e=1}^{e=100} f_e^i}{100} \tag{1}$$

where f_e^i is the value provided by the e^{th} ensemble member at time step i. Then, the estimate of the FR influence is computed by taking simply its variance (FV):

$$FV = \frac{\sum_{i=i_1}^{i_2} (F_r^i - F_r)^2}{i_2 - i_1} \ , \ F_r = \frac{\sum_{i=i_1}^{i_2} F_r^i}{i_2 - i_1 - 1} \tag{2}$$

On the other hand, the internal climate variability is quantified following the procedure described by Maher et al., 2019, in which the associated Internal Variance (IV) in the considered period, from step i_1 to i_2, is computed as:

$$IV = \frac{\sum_{i=i_1}^{i_2} \sum_{e=1}^{e=100} (f_e^i - F_r^i)^2}{100 * (i_2 - i_1 + 1) - 1} \tag{3}$$

The Total Variance (TV) is then the sum of the forced and internal variances:

$$TV = FV + IV \ . \tag{4}$$

and it is defined as:

$$TV = \frac{\sum_{i=i_1}^{i_2} \sum_{e=1}^{e=100} (f_e^i - F_r)^2}{100 * (i_2 - i_1 + 1) - 1} \tag{5}$$

The square root of TV, FV IV, denoted respectively as $\sigma_{TV}, \sigma_{FV}, \sigma_{IV}$ are used to represent the total uncertainty and its components associated with the internal climate variability and the forced response.

Time-of-emergence

The methods for estimating the S/N, which is needed for computing ToE, differ among studies (e.g. Christensen et al., 2007, Giorgi et a., 2009, Hawkins et al., 2012). By considering the global HC edge, the signal is computed as the 30-year running mean $\overline{(\cdot)}$ of the ensemble mean F_r^i and computing its anomaly with respect to the its value in the 1971-2000 period of the historical simulation F_r^{ref}. The noise is estimated as the standard deviation associated to the internal climate variability $\sigma_{\overline{IV^i}}$ considering 30-year long time windows:

$$S/N = \frac{\overline{F_r^i - F_r^{ref}}}{\sigma_{\overline{IV^i}}} . \tag{1}$$

The value of ToE is estimated considering the years when S/N crosses the 0.5 and 1 thresholds.

How are subtropical margins computed?

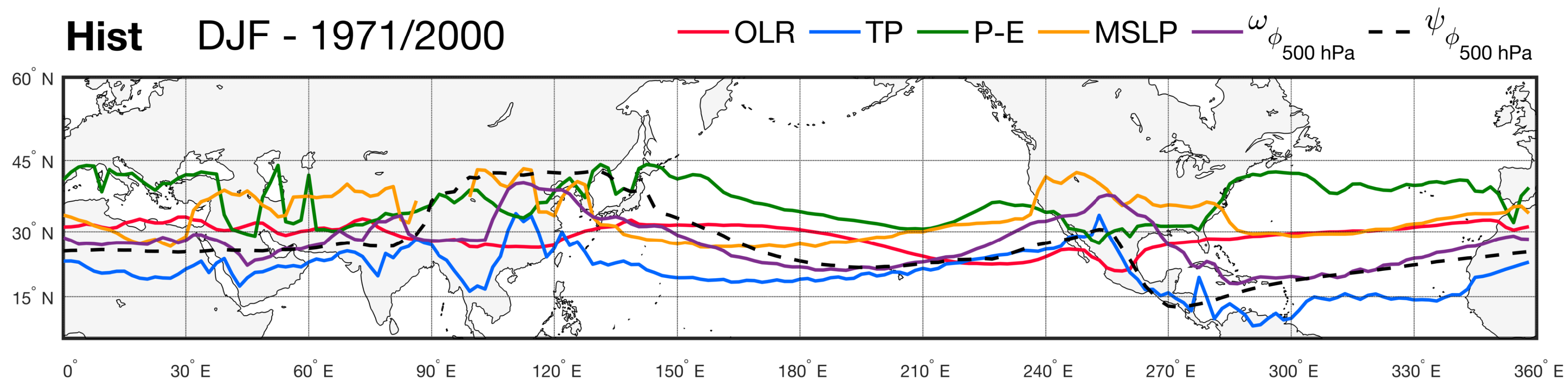

Figure 1: Regional subtropical margins are computed for all indicators and at each longitude within the 5°N - 45°N range.

Regional values:

- **OLR (Outgoing Longwave Radiation)** = latitudes where OLR falls below 250 W/m^2
- **TP (Total Precipitation)** = latitudes of absolute precipitation minima in the subtropics
- **P-E (Precipitation - Evaporation)** = zero-crossing latitudes of P-E
- **MSLP (Mean Sea Level Pressure)** = latitude of absolute maxima of the MSLP, high-pressure ridges in subtropics
- **ω_{ϕ} (vertical velocity associated with the meridional component of the divergent wind)** = latitudes of the absolute vertical velocity maxima at the subsiding branches - 500 hPa
- **Ψ_{ϕ} (streamfunction of the regional meridional overturning circulation)** = zero-crossing latitudes of the streamfunction associated with the poleward limit of the HC in the subtropics - 500 hPa

Hemispheric values = zonal averages of these regional indicators

The role of the forced response on position and trends

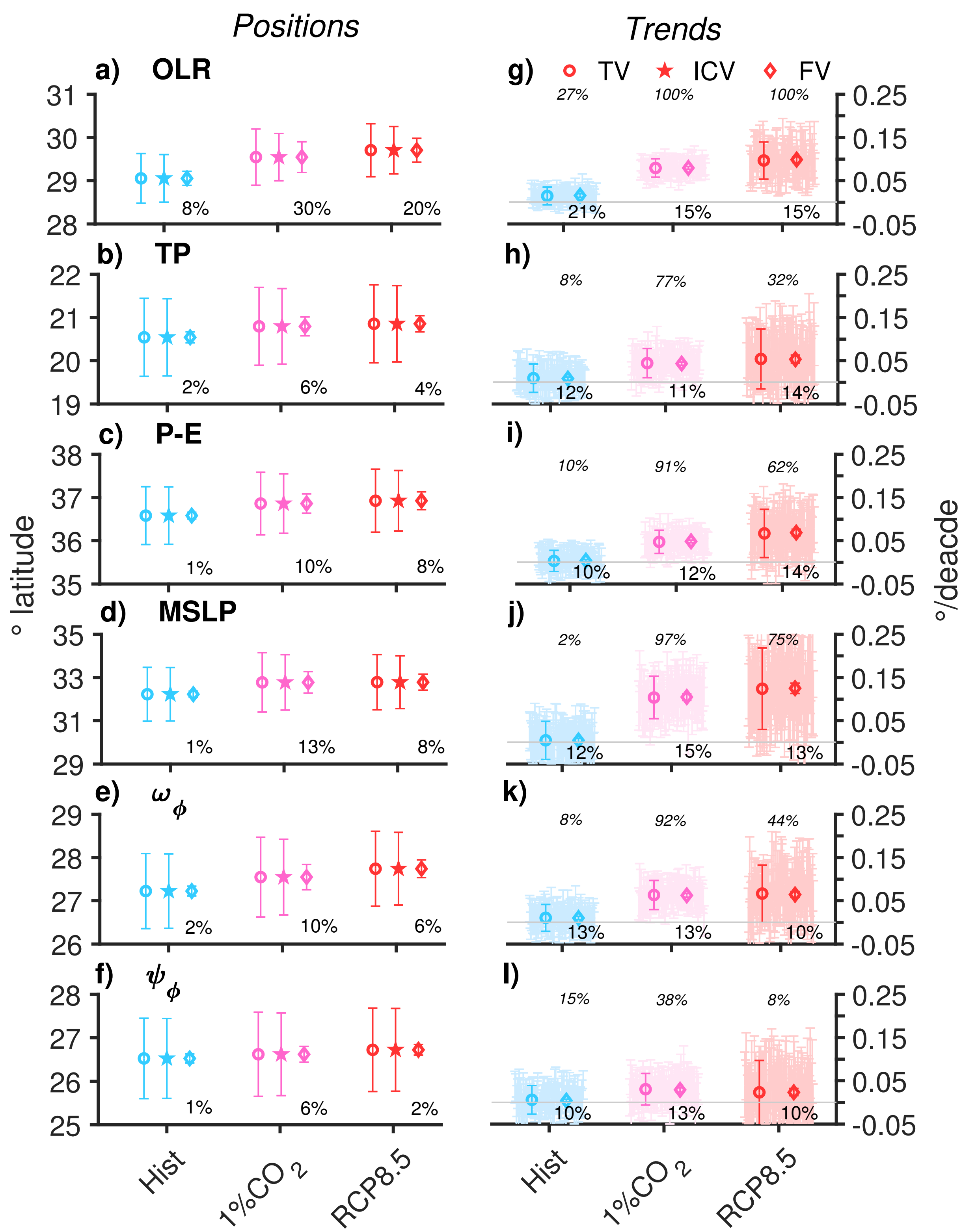

For all zonally averaged indicators and in every experiment, most of the uncertainty in the latitude of the zonally averaged subtropical margins is due to the internal climate variability (ICV, left panels, diamonds).

Most of the ensemble members of the 1%CO2 show trends that are sufficiently large to be statistically significant, while RCP8.5 trends are often not significant for several indicators (namely TP, ω_ϕ, Ψ_ϕ). The percentages annotated in the right panels can be interpreted as probability of detecting a significant trend and are larger than 90% for most indicators only in the 1%CO2.

Figure 2: Positions and trends of the zonally averaged Northern subtropical margins and corresponding uncertainties for the Historical (blue), 1%CO2 (pink) and RCP8.5 (red). Symbols denote total (dots), forced (diamond) and internal (stars) uncertainty (see equation 1). The associated error bars show the corresponding 5th to 95th confidence range. Left panels show the mean value of the time series over the whole period of the experiments. Annotated percentages show the ratio of the forced variance to the total variance. Right panels show the value of the trends (Sen's slopes) considering the whole length of the simulations. Pale colors (light blue, pink and red) denote the uncertainty ranges of the trends of the ensemble members. Annotated values are the percentage of the forced to the total variance (normal font along the bottom axis) and the fraction of members with a statistically significant positive trend (Mann-Kendall test, 95% confidence level, italic font on top of panels).

Time-of-emergence: zonally averaged indicators

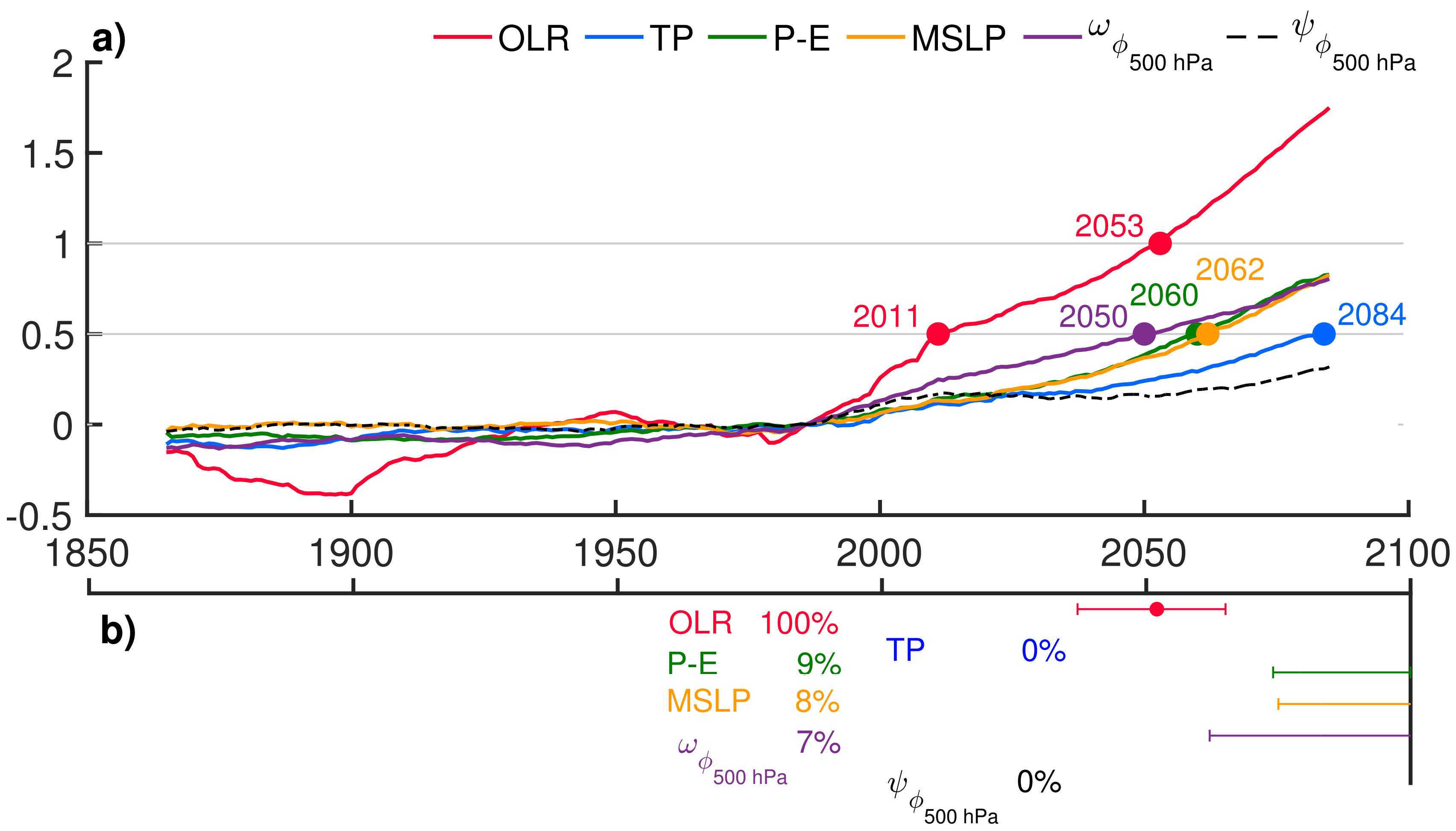

Figure 3: Time of emergence (ToE) of the zonally averaged Northern subtropical margins' shift. Top panel shows the time series of the signal-to-noise ratio S/N of the ensemble mean for different indicators: OLR (red), TP (blue), P-E (green), MSLP (brown), ω_{Φ} (purple) and Ψ_{Φ} (dashed black) at 500 hPa. Time series are obtained joining the Historical and RCP8.5 experiments and consider the 1865-2085 period along which the 31-year running mean is available. Black horizontal lines mark the S/N=0.5 and 1.0 thresholds. Vertical lines mark the year at which the ratio S/N is exceeding the indicated threshold. Bottom panel shows the median ToE of the 100 ensemble members with bars representing the range of the distribution (5^{th} to 95^{th} percentile). The percentage of members with ToE occurring within the end of the 21st century is annotated in the panel. When this percentage is smaller than 50% (95%) the median (the 95^{th} percentile) cannot be computed and they would fall outside the time period shown in the figure.

Time-of-emergence: regional perspective

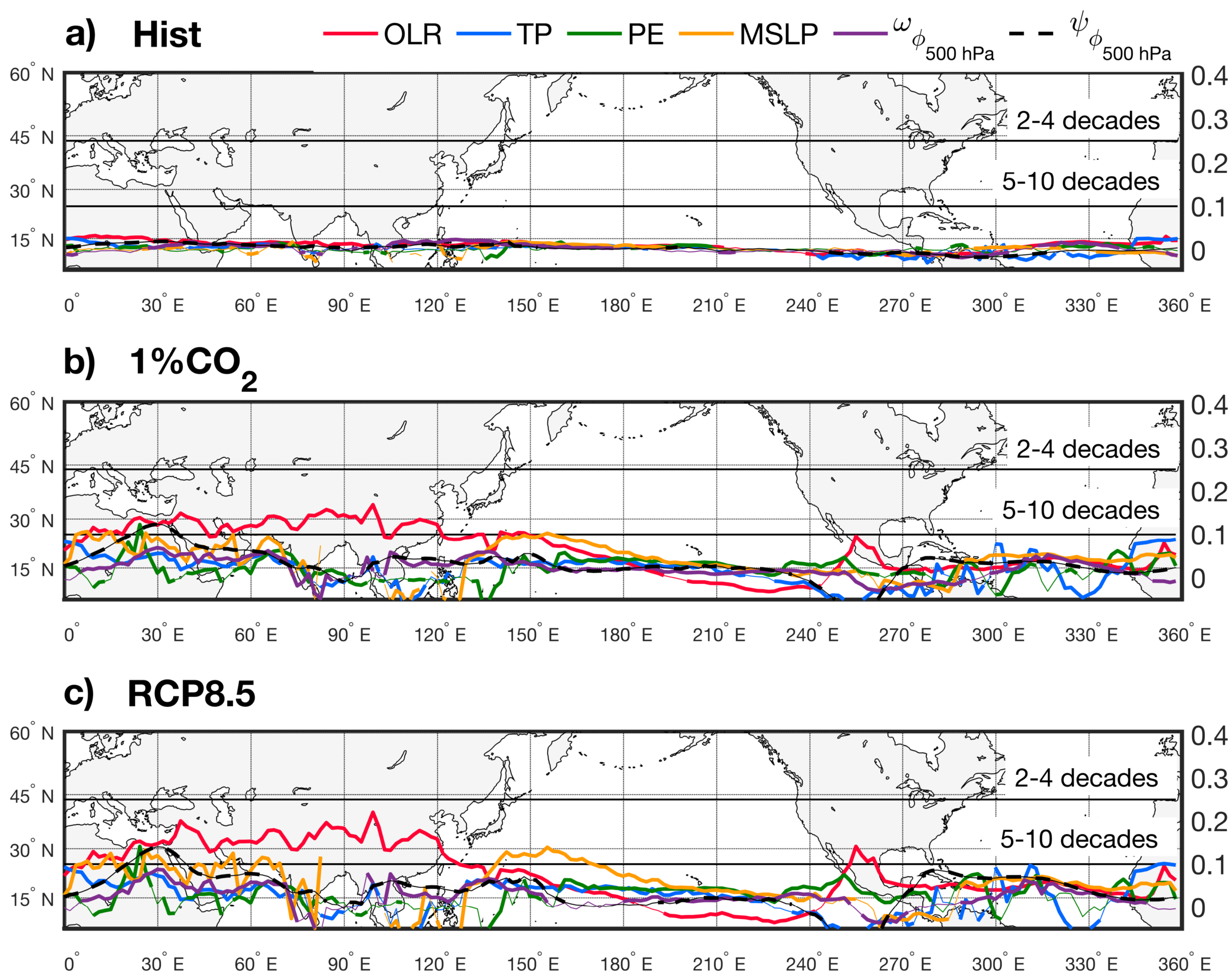

Figure 4: Regional values of the trend of the signal-to-noise ratio. Each panel shows values for different indicators, e.g. OLR (red), TP (blue), P-E (green), MSLP (brown), ω_ϕ (purple) and Ψ_ϕ (dashed black) at 500 hPa for Historical (top), 1%CO2 (middle), RCP8.5 (bottom). The bold parts of the curves indicate the regions where the trend is significant at the 95% level according to the Mann-Kendall test. For values of the trends above the 0.25 and 0.1 black horizontal lines, the signal will exceed the noise in four decades and in one century, respectively.

Conclusions

1. The Northern subtropical margins in DJF are **predominately** affected by the **internal climate variability** in every experiments and among all indicators.
2. **Only a small portion** of the total uncertainty on the expansion rates is attributable to the **forced response**.
3. **The forced signal of northward shift of subtropics will not emerge before the end of the 21st century**, except for the OLR.
4. **Disagreement** among studies that investigated past trends of the Northern Hemisphere HC in observational datasets and reanalyses can be explained by their attempt to assess a **signal that is too small** to be detectable, so that their results reflect mainly **multidecadal fluctuations**.
5. The northward shift of the subtropics has strong regional connotations and only in few areas, e.g. the **eastern Mediterranean, Western Asia and, to a lower extent the Western Pacific**, the anthropogenic climate change signal will emerge from the natural climate variability before the end of the 21st century.

Submitted to Geophysical Research Letters: D'Agostino et al., 2020

Thanks for your attention!

roberta.dagostino@mpimet.mpg.de